Clim. Past Discuss., 2, 519–533, 2006
www.clim-past-discuss.net/2/519/2006/

Climate of the Past Discussions

Climate of the Past Discussions is the access reviewed discussion forum of *Climate of the Past*

Equatorial insolation: from precession harmonics to eccentricity frequencies*

A. Berger[1], **M. F. Loutre**[1], **and J. L. Mélice**[2]

[1]Université catholique de Louvain, Institut d'Astronomie et de Géophysique G. Lemaître, 2 Chemin du Cyclotron, 1348 Louvain-la-Neuve, Belgium
[2]Department of Oceanography, University of Cape Town, Rondebosch 7701, South Africa

Received: 22 June 2006 – Accepted: 9 July 2006 – Published: 24 July 2006

Correspondence to: A. Berger (berger@astr.ucl.ac.be)

*Invited contribution by A. Berger, EGS Milutin Milankovic Medal winner 1994

Abstract

Since the paper by Hays et al. (1976), spectral analyses of climate proxy records provide substantial evidence that a fraction of the climatic variance is driven by insolation changes in the frequency ranges of obliquity and precession variations. However, it is the variance components centered near 100 kyr which dominate most Upper Pleistocene climatic records, although the amount of insolation perturbation at the eccentricity driven 100-kyr period is much too small to cause directly a climate change of ice-age amplitude. Many attempts to find an explanation to this 100-kyr cycle in climatic records have been made over the last decades. Here we show that the double maximum which characterizes the daily irradiation received in tropical latitudes over the course of the year is at the origin in equatorial insolation of not only a strong 100-kyr, but also of a 11-kyr and a 5.5-kyr periods related respectively to eccentricity and to precession.

1 Introduction

The tropics have been long neglected by paleoclimatologists who mostly followed the hypothesis by Murphy (1876), later popularized by Milankovitch (1941), that the driver of the long-term climatic variations is summer in the high northern polar latitudes. For these authors, the progressive build-up of ice sheets requires indeed primarily cool summers in high latitudes, in order to prevent winter snow to melt. But under these conditions, northern latitudes winters are receiving more energy. For example, 114 kyr ago, 70° N in June received 97 $\mathrm{Wm^{-2}}$ less than 126 kyr ago and the equator in December 63 $\mathrm{Wm^{-2}}$ more. This is representing respectively a relative decrease of 18% at 70° N and a relative increase of about the same amount at the equator. This leads to more evaporation in the equatorial regions, a larger latitudinal gradient in the northern hemisphere (remember that if we consider the winter hemisphere, the maximum of the energy received from the Sun is at the equator), a more active transport to the north and possibly more precipitations in polar latitudes. When extended to winter precipitations, the Milankovitch hypothesis is therefore also involving the equatorial and intertropical regions. Many new paleoclimate information indicate that these regions are indeed more important than previously thought. They seem to play an important role in the glacial-interglacial cycles and even in the warming of the last 50 years (see Kerr, 2001, 2003, for a few references).

In this paper, we show an additional reason to believe that the tropics can play an important role in the response of the climate system to the astronomical forcing. This reason is the presence of significant 100-kyr, 11-kyr and 5.5-kyr cycles in the amplitude of the seasonal cycle of the energy that the intertropical regions receive from the Sun, cycles directly related to eccentricity and harmonics of precession.

2 Insolation at the Equator

In contrast with the extra-tropical latitudes, which exhibits a simple maximum of insolation each year, the Sun comes overhead twice a year at each latitude in the intertropical belt. In particular at the equator, the Sun culminates at the zenith at both equinoxes. From classical insolation formula (e.g. Berger et al., 1993) the 24-h mean irradiance at the equator for a given day is given by:

$$\bar{W}_{eq} = \frac{S_a}{\pi}\left(\frac{1 + e\cos(\lambda - \varpi)}{1 - e^2}\right)^2 \cos\delta \tag{1}$$

- S_a is the amount of solar energy received by unit of time on a surface of unit area perpendicular to the Sun rays and situated at the distance a from the Sun. a is the semi-major axis of the Earth's elliptical orbit around the Sun. It is an invariant in celestial mechanics contrary to the so-called solar constant S_0, which is defined at the mean distance r_m from the Earth to the Sun. On an energy point of view, r_m is given by

$$r_m^2 = a^2\sqrt{1 - e^2}$$

where e is the eccentricity of the Earth's orbit. r_m and therefore S_0 are varying with e as:

$$S_0 = \frac{S_a}{\sqrt{1 - e^2}} \tag{2}$$

In the astronomical theory of paleoclimates, the energy output from the Sun is assumed to remain constant over the last millions of years and therefore S_a is a constant taken to be 1368 $\mathrm{Wm^{-2}}$ in our calculation.

- The declination δ is related to the true longitude of the Sun by

$$\sin\delta = \sin\lambda\ \sin\varepsilon \tag{3}$$

ε being the obliquity and λ identifying the calendar days.

- ϖ is the longitude of the perihelion. Its numerical value is obtained by adding 180° to $\tilde{\varpi}$ calculated from Berger (1978) (see Berger et al., 1993, for more explanations).

- The distance from the Earth to the Sun, r, δ and λ are assumed to be constant over one day.

From Eq. (1), the energy received at the equinoxes (δ=0; λ=0 for the spring equinox, SE, or π, for the fall equinox, FE) and solstices ($\delta=\varepsilon$ or $\lambda=\frac{\pi}{2}$ for summer solstice, SS and $\delta=-\varepsilon$ or $\lambda=\frac{3\pi}{2}$ for winter solstice, WS) can be calculated.

For the present-day with e=0.0167, ϖ=282° and ε=23°27′, SE=439 $\mathrm{Wm^{-2}}$, SS=387 $\mathrm{Wm^{-2}}$, FE=433 $\mathrm{Wm^{-2}}$ and WS=413 $\mathrm{Wm^{-2}}$ leading to a seasonal contrast of 52 $\mathrm{Wm^{-2}}$ (SE-SS) Because of precession, the insolation at SE will alternatively be larger and lower than at FE (see Fig. 1). The same holds for the insolation at SS and

WS. However, strictly speaking, the insolation values at SE and FE on one hand, and at SS and WS on the other hand, do not provide the absolute maxima and minima over the year. Indeed, these extrema do not occur exactly at the equinoxes and solstices because the Earth-Sun distance modulates the effect of δ in the course of the year.

Fortunately however, the error made by assuming that the maximum is occurring at one of the equinoxes (Fig. 2) and the minimum (Fig. 3) at one of the solstices remains small. For example, assuming that the summer solstice occurs at the perihelion maximizes the energy received at that particular time. At 198 kyr BP, $\varpi \simeq 90^\circ$ and the absolute maximum arises in August (with 451 Wm^{-2}), but is only 13 Wm^{-2} larger than the insolation at the fall equinox (438 Wm^{-2}). This means that the error assuming that the maximum occurs at FE is less than 3%. As the minimum is actually at WS (364 Wm^{-2}), the real seasonal difference amounts to 87 Wm^{-2}, instead of 74 Wm^{-2} if FE-WS is used. Although the error on the seasonal difference reaches 15%, it does not affect the spectral characteristics of the long-term variations of this seasonal difference calculated between the maximum and the minimum values. So for an analytical calculation we will assume that the maximum is occurring at the equinoxes (SE, spring, or FE, fall) and the minimum at the solstices (SS, summer, or WS, winter).

If we assume e and ε constant over a precessional period, it is easy to see that:

$$\begin{array}{lll} \text{SE is maximum} & \text{for} & -90^\circ \le \varpi \le 90^\circ \\ \text{FE is maximum} & \text{for} & 90^\circ \le \varpi \le 270^\circ \\ \text{SS is minimum} & \text{for} & 180^\circ \le \varpi \le 360^\circ \\ \text{WS is minimum} & \text{for} & 0^\circ \le \varpi \le 180^\circ \end{array} \quad (4)$$

In these conditions, the seasonal contrast measured by Δ=Max (SE,FE)–min (SS,WS) (Fig. 4) is equal to:

$$\begin{array}{lll} \text{SE–WS} & \text{for} & 0^\circ \le \varpi \le 90^\circ \\ \text{FE–WS} & \text{for} & 90^\circ \le \varpi \le 180^\circ \\ \text{FE–SS} & \text{for} & 180^\circ \le \varpi \le 270^\circ \\ \text{SE–SS} & \text{for} & 270^\circ \le \varpi \le 360^\circ \end{array} \quad (5)$$

(let us recall that the perihelion coincides with the spring equinox for $\varpi=0^\circ$, with the summer solstice for $\varpi=90^\circ$, with the fall equinox for $\varpi=180^\circ$ and with the winter solstice for $\varpi=270^\circ$).

This is again an approximation because the insolation at the equinoxes and solstices are also functions of e and ε. This approximation is actually used to allow an easy analytical range of ϖ values to be calculated (in reality, the boundaries of these ranges are not constant in time, varying slightly around 0, 90, 180 and 270°). However, calculations over the last and next million years show that Δ is practically equivalent to the real seasonal amplitude of insolation at the equator.

The most striking feature of Fig. 5 (top panel), reproducing the long term variations of Δ over the last 1 Myr is the significant eccentricity cycles (both the 100 and the 400-kyr) dominating its long-term variations. In addition, a clear and significant 5-kyr period is present with a large amplitude (~10 Wm^{-2}) for large values of e and a small one for low values of e. The explanation of the high frequency variability finds an origin similar to the half-precession cycle discussed in Berger and Loutre (1997). It was indeed stressed that, although the insolation at the equinoxes follows the climatic precession pattern, the existence of a double maximum at the equator offers the possibility of generating a half-precession cycle (~11 kyr) if the climate system is supposed to respond automatically to the largest value of the two. This is clearly seen in Figs. 2 and 3. If now, the largest seasonal amplitude, Δ, is supposed to drive the climate system behaviour, the two maxima and the two minima are involved. Δ(=Max(SE,FE)–min(SS,WS)) is therefore equal to the largest value of the four following parameters: SE–WS, FE–WS, FE–SS, SE–SS (Fig. 5). This means that, according to Eq. (4), a one-fourth-precession cycle is generated. The signal of obliquity, which comes from SS and WS is actually weak compared to the harmonics of precession because ε is not a purely periodic function, but instead is equal to a constant plus a series of periodic terms, the most important having a period of 41 kyr. Therefore $\cos\varepsilon$ can be considered as a constant to the first order of approximation.

As all values at the equinoxes and solstices are principally a function of precession, their amplitude is modulated by eccentricity (which is therefore the envelope of insolation). Therefore, through the procedure of the maximum and minimum selection, this envelope becomes naturally the carrier of the "seasonal" contrast of insolation at the equator leading to the existence of eccentricity in the spectra.

As a consequence, the spectrum of Δ shows the 400, 100, 41, ~10 and ~5-kyr quasi-periods, all being significant, with a maximum centred at ~100 and ~5-kyr (Fig. 5 middle and lower panels). The characteristic of their behaviour are the same as those of eccentricity and precession discussed in Berger et al. (1998).

As this double culmination of the Sun at the zenith is true for the whole intertropical belt, it is interesting to see if this equatorial features holds for all the other intertropical latitudes. Actually, the spectra for these latitudes continue to show all the frequencies but the amplitude of the 100, 11 and 5.5 kyr-cycles decreases rapidly when getting away from the equator. For example, at 5° N, the largest spectral amplitude is related to precession, followed by eccentricity, then the obliquity and the 11 kyr. The harmonic 5.5 kyr is still present but its amplitude is 10 times less than the amplitude of the 11-kyr harmonic.

3 Conclusions

More papers are now questioning whether the origin of the glacial-interglacial cycles lies in the high latitudes. They show some evidence that the low latitudes are maybe as or more important than the high latitudes. For example, Hagelberg et al. (1994) found climate variability at periods from 10 to 12 kyr (equal to harmonics of precession) in three locations for the late Pleistocene. They concluded that this variability may derive from high sensitivity of the tropics to summer time insolation in both hemispheres. An amplified response of tropical precipitation and temperature may then be transmitted to high latitudes in the Atlantic via advective transport, a mechanism appearing consistent with their observations. McIntyre and Molfino (1996) suggested from spectra

of high resolution records from the equatorial Atlantic spanning the last 50 kyr, that climatic changes in high polar latitudes may be caused by events that occur in low latitudes. Turney et al. (2004) found semi-precessional periods and suggested that climate variations in the tropical Pacific Ocean exerted an influence on North Atlantic climate through atmospheric and oceanic teleconnections. Thibault de Garidel-Toron et al. (2005) inferred from high resolution records of sea-surface temperature from the Pacific warm pool that the temperature contrast across the equatorial Pacific Ocean might have had a significant influence on the mid-Pleistocene climate transition. But the most significant proof of the existence of half-precessional cycles comes from the Chinese loess. According to Sun and Huong (2006), the well-defined half-precessional cycle found in magnetic susceptibility and particle size records from the north western Loess Plateau in China is a direct response of the low-latitude insolation forcing through its modulation on the East Asian Summer monsoon. It might be expected that, if resolution permits, the 5.5-kyr cycle might be found and used as a relevant test of the real role played by the tropics.

These are a few examples only and more must be made to show that indeed the tropics can play a leading role in generating long-term climatic variations. In this paper we have demonstrated that the spectrum of the insolation forcing at the equator is as informative than in the high polar latitudes where only the precession and obliquity signals are present. The double insolation maximum and minimum arising in the tropical regions in the course of one year, which is at the origin of the 100 and 5.5 kyr cycles might explain some of the important features of the climate system and environment over the Pleistocene and the Holocene, like it is suggested also by Lorenz et al. (2006) and Reuning et al. (2006) for example.

References

Berger, A.: Long-term variations of daily insolation and Quaternary climatic changes, J. Atmos. Sci., 35(12), 2362–2367, 1978.

Berger, A., Loutre, M. F., and Tricot, Ch.: Insolation and Earth's orbital periods, J. Geophys. Res., 98(D6), 10 341–10 362, 1993.
Berger, A. and Loutre, M. F.: Intertropical latitudes and precessional and half-precessional cycles, Science, 278(5342), 1476–1478, 1997.
Berger, A., Loutre, M. F., and Mélice, J. L.: Instability of the astronomical periods from 1.5 Myr BP to 0.5 Myr AP, Palaeoclimates, Data and Modelling, 2(4), 239–280, 1998.
De Garidel-Thoron, Th., Rosenthal, Y., Bassinot, F., and Beaufort, L.: Stable sea surface temperatures in the Western Pacific warm pool over the past 1.75 million years, Nature, 433(7023), 294–298, 2005.
Hagelberg, T. K., Bond, G., and de Menocal, P.: Milankovitch band forcing of sub-Milankovitch climate variability during the Pleistocene, Paleoceanography, 9(4), 545–558, 1994.
Hays, J. D., Imbrie, J., and Shackleton, N. J.: Variations in the Earth's orbit: pacemaker of the Ice Ages, Science, 194, 1121–1132, 1976.
Kerr, R. A.: The Tropics return to the climate system, Sciences, 292(5517), 660–661, 2001.
Kerr, R. A.: Tropical Pacific a key to deglaciation, Science, 299(5604), 183–184, 2003.
Lorenz, S. J., Kim, J. H., Rimbu, N., Schneider, R. R., and Lohmann, G.: Orbitally driven insolation forcing on Holocene climate trends: evidence from alkenone data and climate modelling, Paleoceanography, 21, PA1002, doi:10.1029/2005PA001152, 2006.
McIntyre, A. and Molfino, B.: Forcing of Atlantic equatorial and subpolar millennial cycles by precession, Science, 274(5294), 1867–1870, 1996.
Milankovitch, M.: Kanon der Erdbestrahlung und seine Anwendung auf das Eiszeitenproblem. Royal Serbian Sciences, Spec. pub. 132, section of Mathematical and Natural Sciences, vol. 33, pp. 633, Belgrade, 1941; ("Canon of Insolation and the Ice Age problem", English Translation by Israël Program for Scientific Translation and published for the U.S. Department of Commerce and the National Science Foundation, Washington D.C., 1969, and by Zavod za Udzbenike I nastavna Sredstva in cooperation with muzej nauke I technike Srpske akademije nauka I umetnosti, Beograd, 1998).
Murphy, J. J.: The glacial climate and the polar ice-cap, Quarterly Journal Geological Society, 32, 400–406, 1876.
Reuning, L., Reijmer, J. J. G., Betzler, Ch., Timmermann, A., and Steph, S.: Sub-Milankovitch cycles in periplatform carbonates from the early Pliocene Great Bahama Bank, Paleoceanography, 21, PA1017, doi:10.1029/2004PA001075, 2006.
Sun, J. and Huang, X.: Half-precession cycles recorded in Chinese loess: response to low-

latitude insolation forcing during the Last Interglaciation, Quaternary Science Reviews, 25(9–10), 1065–1972, 2006.
Turney, C. S. M., Kershaw, A. P., Clemens, S. C., Branch, N., Moss, P. T., and Fifield, L. K.: Millennial and orbital variations of El Nino/Southern oscillation and high-latitude climate in the last glacial period, Nature, 428(6980), 306–310, 2004.

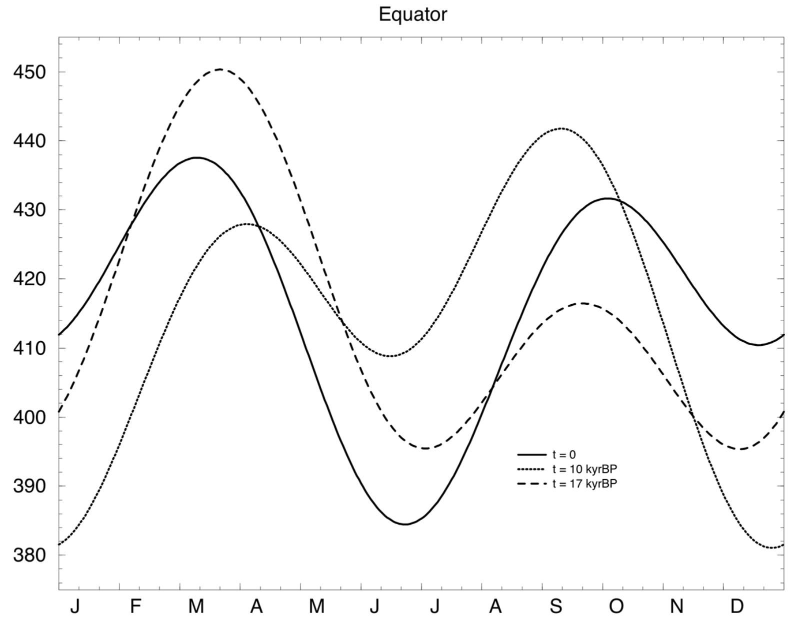

Fig. 1. Seasonal cycle of insolation at the equator at present (full line), at 10 kyr BP (dotted line) and at 17 kyr BP (dashed line). Units are Wm^{-2}.

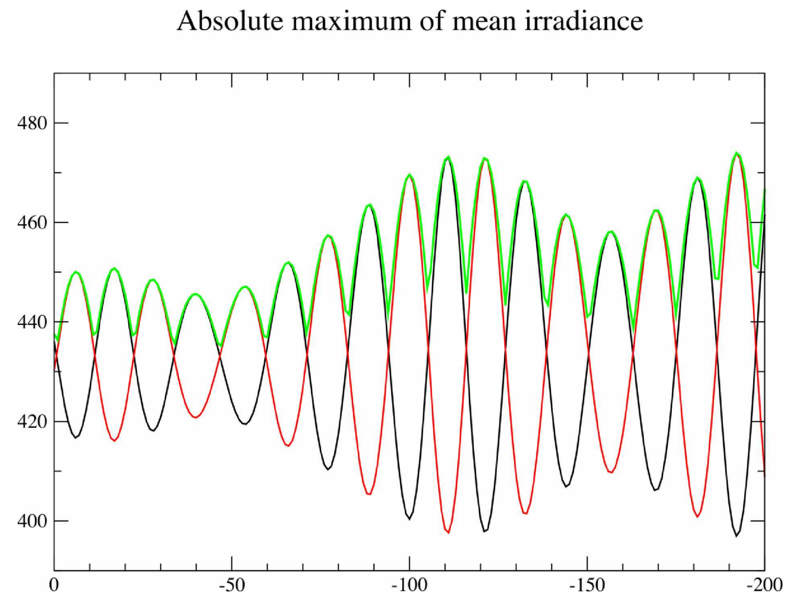

Fig. 2. Time evolution over the last 200 kyr of the 24-h mean irradiance at the equator at spring equinox (black curve) and at autumn equinox (red curve). The time evolution of the maximum of these two series is drawn in green. Units are Wm^{-2}.

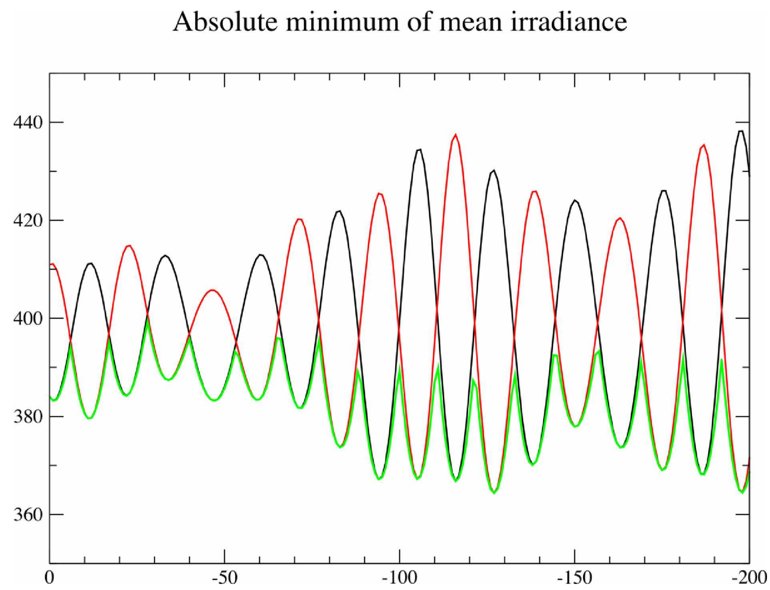

Fig. 3. Time evolution over the last 200 kyr of the 24-h mean irradiance at the equator at summer solstice (black curve) and at winter solstice (red curve). The time evolution of the minimum of these two series is drawn in green. Units are Wm^{-2}.

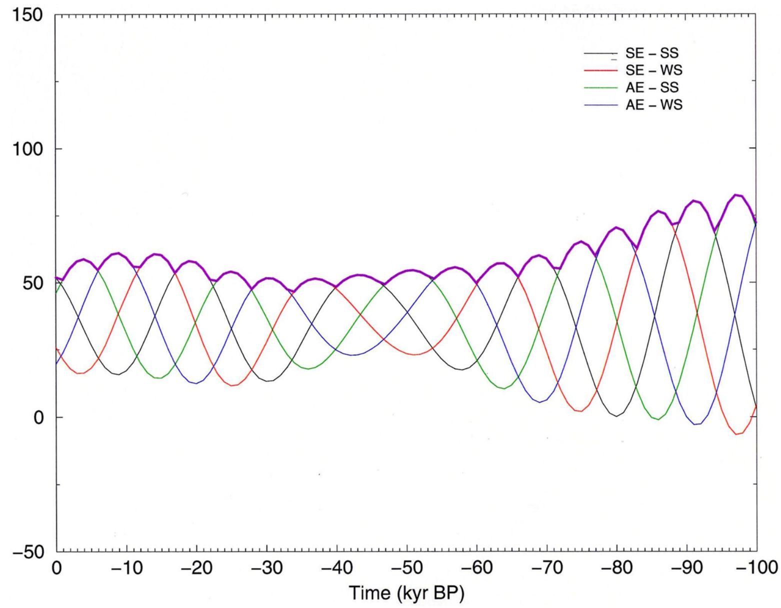

Fig. 4. Time evolution over the last 100 kyr of the amplitude of the 24-h mean irradiance at the equator between spring equinox and summer solstice (black), spring equinox and winter solstice (red), autumn equinox and summer solstice (green) and autumn equinox and winter solstice (blue), and the largest amplitude in the seasonal cycle (purple). Units are Wm^{-2}.

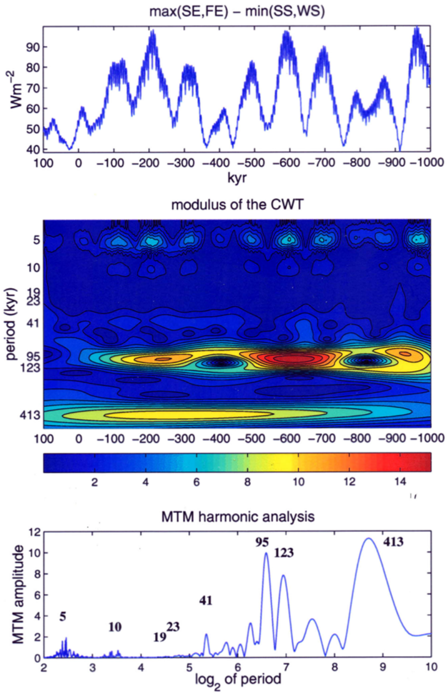

Fig. 5. From top to bottom: (top) time evolution between 1000 kyr BP and 100 kyr AP of the maximum of the amplitude of the seasonal cycle of the 24-h mean irradiance at the equator, (centre) the modulus of the wavelet transform of the signal on top, (bottom) amplitude in the multi taper analysis of the signal on top.